Assessing the Portion of the Crack Length Contributing to Water Sorption in Concrete Using X-ray Absorption

Pease, Bradley Justin; Couch, Jon; Geiker, Mette Rica; Stang, Henrik; Weiss, Jason

Published in:
ConcreteLife'09: Second International RILEM Workshop on Concrete Durability and Service Life Planning

Publication date:
2009

Document Version
Early version, also known as pre-print

Pease, B., Couch, J., Geiker, M., Stang, H., and Weiss, J., "Assessing the Portion of the Crack Length Contributing to Water Sorption in Concrete Using X-Ray Absorption," Proceedings of ConcreteLife'09: Second International RILEM Workshop on Concrete Durability and Service Life Planning, Haifa, Israel, September 2009

ASSESSING THE PORTION OF THE CRACK LENGTH CONTRIBUTING TO WATER SORPTION IN CONCRETE USING X-RAY ABSORPTION

Brad Pease[1], Jon Couch[2], Mette Geiker[1], Henrik Stang[1], and Jason Weiss[2]

(1) Department of Civil Engineering, Technical University of Denmark, Lyngby, Denmark

(2) School of Civil Engineering, Purdue University, West Lafayette, IN, USA

Abstract

While it is generally known that cracks accelerate fluid movements, there is a need to quantify how cracks influence the controlling transport mechanism(s) for more accurate service life modeling. This paper describes an experimental approach using x-ray absorption measurements to quantify the influence of cracks with varying width and length on water sorption in concrete. Concrete wedge splitting specimens, conditioned to 50% relative humidity, were loaded to varying crack openings. Water sorption was monitored for ponded specimens with varying crack widths and lengths by taking multiple x-ray absorption measurements over time. The effect cracks have on sorption is discussed and compared to the behavior of pristine concrete. In addition, the maximum water sorption depth after one hour of exposure is compared to crack lengths determined by the cracked hinge model.

1. INTRODUCTION AND MOTIVATION

It is generally accepted that the presence of cracks in concrete allow for a more rapid ingress of aggressive substances, possibly leading to durability issues and shortened service life. To date however, few quantitative results relate the controlling processes of cracking and ingress; namely linking fracture mechanics approaches with fluid or ion transport behavior in cementitious materials.

In this paper, concrete wedge splitting test (WST) specimens were used to measure fracture parameters and ingress behavior. Elastic modulus, tensile strength and the cohesive law for concrete fracture were estimated via inverse analysis. Water sorption was monitored in cracked, non-saturated specimens using an x-ray camera. The comparisons indicate that cracks consist of two portions, an 'apparent crack' – behaving approximately like a free surface for ingress – and an 'inhibited crack.'

2. EXPERIMENTAL APPROACH

This paper outlines initial results from an experimental study which intends to quantify the effect cracking has on the ingress of water and aggressive substances into concrete. In this research program concrete WST specimens were cast, cured, conditioned, and placed under mechanical loading to introduce cracks with varying lengths and widths. The cracked WST

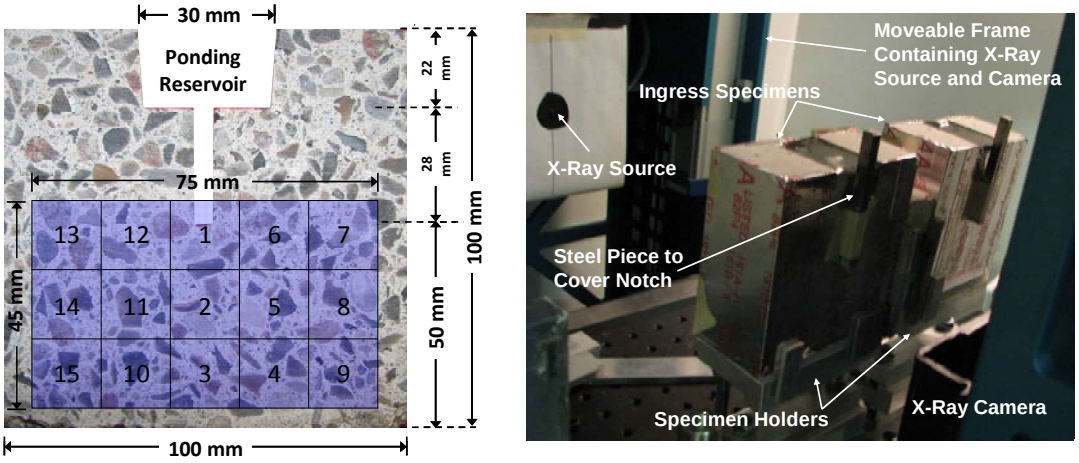

(a) *(b)*

Figure 1. *(a)* The WST specimen geometry and details on location of x-ray images and *(b)* x-ray system setup including moveable frame, x-ray source and camera, and specimen holders.

specimens were used to monitor water sorption via non-destructive x-ray measurements. Details on the experimental approach are given in the following sections.

2.1 Mixture Proportions and Specimen Preparation

Concrete WST specimens, with dimensions shown in Figure 1*(a)* and thickness of 100 mm, were prepared using a water-to-cement ratio of 0.50 and a cement content of 330 kg/m^3. Aalborg White© portland cement was used with chemical composition consisting of 78.8% C_3S, 10.5% C_2S, 4.9% C_3A, 1.0% C_4AF, 0.6% MgO, 2.1% SO_3, and an Na_2O equivalent alkali content of 0.19%. Aggregate consisted of washed Class E 0-4 mm sea-sand, and washed Class A 4-8 mm sea-gravel (in accordance with [1]). The concrete contained 72.5% aggregate by volume, 776 kg/m^3 fine aggregate and 1103 kg/m^3 coarse aggregate.

The concrete was mixed using a standard pan mixer with a 120 L capacity. The fine and coarse aggregate were first mixed dry for 1 minute, followed by 3 minutes mixing with one third of the mixing water. Mixing was stopped for 2 minutes prior to adding cement and mixing for 1 minute. The remaining water was then added and mixing continued for 3 minutes after addition of water. The mixer was then opened and the pan and blades were scraped, followed by 1 additional minute of mixing.

The concrete was placed and vibrated into molds and allowed to cure, covered by plastic, for 24 hours at ~20°C. WST specimens were cast in special molds to position the ponding reservoir vertically at the mold wall (i.e., the mold has cross-section shown in Figure 1*(a)* when viewed from above). Upon demolding, specimens were sealed with multiple layers of plastic, placed in sealed plastic storage containers, and stored at 20°C ±1°C for 6 days prior to storing in an oven at 45°C ±1°C until reaching a maturity age of ~1 year (using an activation energy 33.5 kJ/mol [2]). During the accelerated curing phase water was placed in the oven to minimize moisture loss in the sealed specimens. After curing, a 28 mm deep notch was cut using a wet saw, followed by halving the specimen perpendicular to the notch, resulting in two separate 50 mm thick specimens. The specimens were then allowed to dry in a 50% ±2% relative humidity, 23°C ±1°C chamber for 18 months prior to testing.

Load was applied to WST specimens via a rigid wedge and roller bearing to varying pre- and post-peak load conditions to induce crack growth. Additional information on the WST procedure is available in literature [3]. Three companion specimens were tested to failure for average fracture parameter determinations as described below. Water sorption was monitored for WST specimens that were unloaded, loaded to peak load and cracked with crack mouth opening displacements (CMOD's) of 0.10, 0.15, 0.20, and 0.40 mm. In order to maintain the induced crack openings in post-peak load specimen, loading was paused at the desired CMOD and 2 hard plastic shims were placed into the notch prior to load removal. Minimal CMOD recovery occurred in post-peak load specimens when using the wedges (~0.01 mm). Immediately after unloading, the specimens were sealed with aluminum tape on all sides, except the top, in order to create a reservoir for ponding. The tape was smoothed to insure a tight seal with the specimen surface (to avoid leakage). Specimens were then stored at 50% ±2% relative humidity and 23°C ±1°C until x-ray absorption testing.

2.2 Inverse Analysis of the Cracked Hinge Model

As previously mentioned, three WST specimens were used to determine fracture parameter. The WST can be used to determine the cohesive law, elastic modulus and tensile strength for a material through inverse analysis utilizing an appropriate model (e.g., minimizing difference between model calculations and experimental results by altering mechanical parameters). The inverse analysis procedure developed in [3] and further modified in [4] applies to the cracked hinge model [5,6] and was implemented on the WST geometry as shown in Figure 2. Figure 2*(a)* shows the crack hinge model (CHM) which simulates the area directly surrounding a propagating crack in the WST specimen using the stress profile shown in Figure 2*(c)*. The cracked hinge is joined to the remaining area via rigid boundaries which are allowed to translate and rotate as indicated in Figure 2*(b)*. The rigid boundaries seamlessly join the bulk (uncracked) specimen, where the behavior is controlled by Hooke's Law.

An inverse analysis procedure developed in [4] was used to estimate material properties (it was found that a cohesive law with three slopes provided the best fit). Additionally, the CHM provides an estimate of the crack profile at the various conditions considered for ingress testing. As show in [7] the angular deformation, φ (Figure 2*(b)*) of the crack hinge is determined during the inverse analysis, and can be used to calculate the crack profile for a particular load. Estimated profiles compared reasonable well to crack profiles determined using photogrammetry [7].

2.3 X-ray Absorption Measurement Technique

Several researchers have used x-ray absorption measurements to monitor fluid or moisture movements in cementitious materials in a non-destructive manner [8,9,10,11,12]. Here, x-ray absorption measurements in a GNI x-ray system located at Purdue University [13] were used to monitor water sorption in WST specimens. As shown in Figure 1*(b)*, the WST specimens were place between the x-ray source and camera, with 500 mm from the source to camera, and 392 mm from source to specimen. The x-ray source and camera are housed in a programmable, moveable frame (Figure 1*(b)*). Through trials, x-ray source energy levels of 75 keV and 100 μA were determined adequate for the specimen thickness used. X-ray absorption behavior varies with density changes caused by addition of water to the concrete. The x-ray absorption of the specimens was measured using a 25 mm x 25 mm x-ray camera.

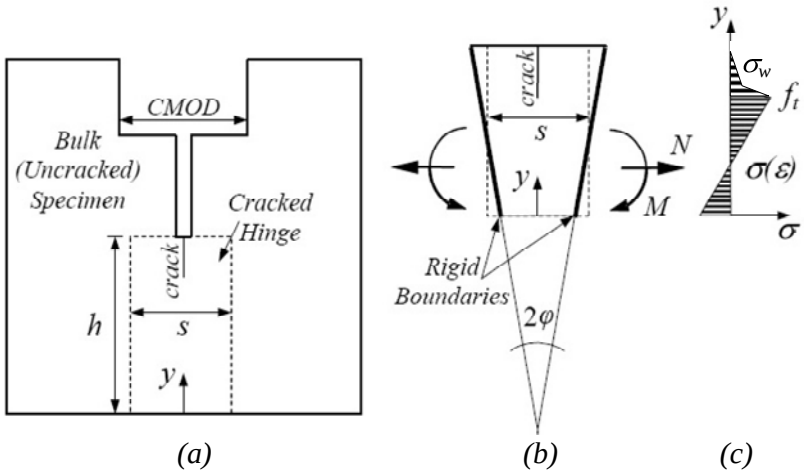

Figure 2. *(a)* The WST specimen with the cracked hinge model applied, *(b)* Loading and deformation of the hinge (after [8]), and *(c)* the assumed stress distribution (after [11]).

The camera consists of NaI crystals, which emit visible light when impacted by an x-ray photon; and a 252x256 pixel photomultiplier, which records the number of light events at each pixel over a set period of time (5 seconds used here). These light events are referred to as counts. Images from the x-ray camera were taken over the area of the specimen indicated in Figure 1*(a)* using 15 mm movements, proceeding in the order indicated. At each measurement location, 10 images were captured, cropped, de-speckled, averaged, tiled, shifted, and analyzed using a batch code written in ImageJ [14,15,16]. Reference measurements were initially taken on the dry specimens. After the reference measurements were taken the specimens were ponded with tap water. Additional x-ray measurements were taken immediately after the introduction of water (i.e., 1 minute) as well as 1, 2, 3, 4, 6 and 24 hours after water addition.

It is important to note the differences in data provided by an x-ray camera and an x-ray detector. In [8,9,10,11,12] x-ray detectors were used to measure x-ray absorption at a single point (or small area) in a specimen over a period of time. Spatial data was provided by repeating measurements at many locations, moving the x-ray source and detector relative to the specimen. In [12], an x-ray detector was used to observe water sorption in WST specimen over a comparable sized area using a grid of 91 measurement points (13x7 pixels). Here, using an x-ray camera at 15 measurement areas (Figure 1*(a)*) a grid of 695506 points were monitored (1057x658 pixels). The measurement process took approximately 28 minutes.

An empirical water absorption index (*ABS)* was computed using the x-ray images and the algorithm shown in Equation 1

$$ABS = \frac{\left(I_{x,y}\right)_{Dry} - \left(I_{x,y}\right)_{Wet,i}}{\left(I_{x,y}\right)_{Dry} - \left(I_{x,y}\right)_{Wet,n}} \cdot 100\% \qquad \text{Equation 1}$$

where $(I_{x,y})_{Dry}$ and $(I_{x,y})_{Wet,i}$ are the counts in each pixel of the dry image and wet image taken at each individual (i hours) and final measurement time (n = 6 hours). After 6 hours of ponding, the initial moisture front had passed through the measurement area. While the entire pore structure is not saturated after 6 hours, little change in x-ray absorption was seen after

this time. The normalization to the 6 hour measurement accounts for differences in counts that occur due to variations in paste content in the concrete [12].

3. EXPERIMENTAL RESULTS

3.1 Inverse Analysis and Crack Profile Estimation

Figure 3*(a)* shows the average cohesive law determined through inverse analysis of three WST specimens loaded to failure. The critical crack width (minimum width causing a stress-free crack) was found to be 0.66 mm. The elastic modulus and tensile strength were estimated at 31.4 GPa and 3.2 MPa, respectively.

Using these material parameters and the angular deformation of the cracked hinge, φ shown in Figure 2*(b)*, the crack profile can be calculated [6]. The estimated crack profiles for the CMOD's used in this study are shown in Figure 3*(b)*, with the crack length (in terms of depth into WST specimen) versus CMOD response shown in Figure 3*(c)*. At peak loading a crack length of 24.5 mm was estimated, although with narrow crack opening displacements (Figure 3*(b)*). Figures 3*(b)* and *(c)* show crack length increases with larger CMOD's to a length of 45.2 mm for the 0.40 mm CMOD specimen. Figure 3*(c)* indicates that initially crack length increases rapidly at smaller CMOD's (< 0.15 mm) followed by more stable crack growth. In addition, as the CMOD increases tractions reduce according to the cohesive law resulting in the slope change in crack profiles shown in Figure 3*(b)*.

Photogrammetry measurement of the crack profile at the WST specimen surface have been shown to agree well with estimated crack profiles, especially with post-peak loading [7]. It is important to note that the CHM uses the cohesive law (Figure 3*(a)*) to simplify fracture processes of concrete and assumes a single discrete crack with an idealized shape. However, in actuality the crack opening displacement at a particular depth of the concrete is likely comprised of coalesced cracks, crack branches, and/or isolated microcracks. As discussed in the following sections, the crack behavior (coalesced, branched, isolated) may have implications on ingress behavior.

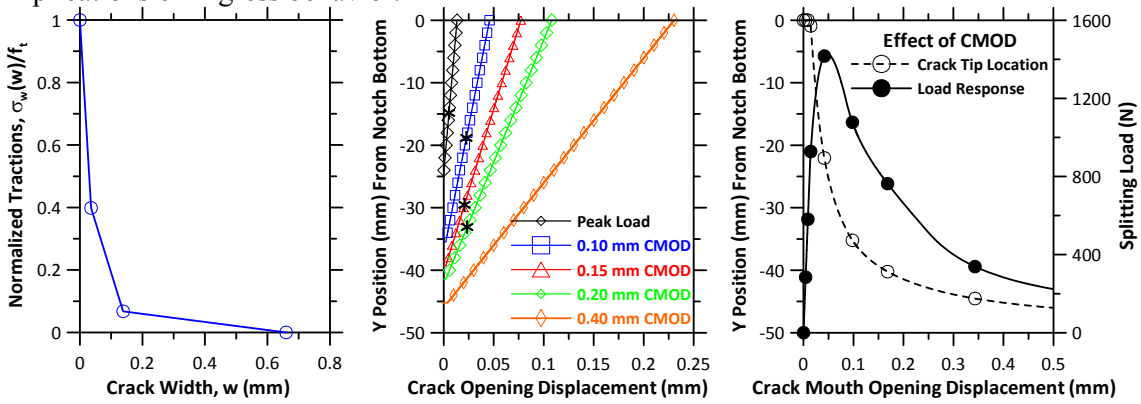

Figure 3. *(a)* The cohesive law from inverse analysis, *(b)* crack profiles from CHM with asterisks indicating maximum sorption depth after 1 hour of ponding, and *(c)* the effect of CMOD on crack length from the notch bottom (dash line) and load response (solid line).

3.2 Moisture Ingress Measurements

Figure 4*(a)* shows a contour plot of the moisture ingress (the *ABS* ratio) after 1 hour of water ponding for the 0.15 mm CMOD specimen, as calculated from Equation 1. The black rectangle indicates the location of the notch. Water traveled rapidly through cracks resulting in an accelerated ingress behavior into the depth of the WST specimens. Similar accelerated ingress behavior was seen for all cracked specimen after 1 hour of water exposure as illustrated in Figure 4*(b)*.

Using the 75% *ABS* ratio contour lines from the x-ray measurements taken 1 hour after water exposure, the lateral sorption was determined at varying depths in the specimens (Y-position). The *ABS* ratio contour lines were exported to AutoCAD and the total lateral sorption was measured at various depths (0.50 mm vertical steps used starting from 5 mm above notch). The lateral sorption was averaged at each depth and the results are shown as sorption profiles in Figure 4*(b)*. The 0.40 mm CMOD specimen was not included as rapid moisture ingress occurred in the vertical direction beyond the measurement area. The average lateral sorption from 0 to +5 mm (y position) indicates the sorption behavior from the sides of the notch.

The notch in the WST specimens may be considered a free surface for water sorption. Similar average lateral sorption distances were observed in the cracked specimens above and below the notch bottom to a given depth (Figure 4*(b)*). This indicates a free surface may exist below the notch bottom in the cracked WST specimens, possibly in the form of a coalesced crack. The maximum sorption depth into the cracked WST specimens after 1 hour of water exposure (from Figure 4*(b)*) is plotted over the corresponding crack profile in Figure 3*(b)* as asterisks (except for CMOD 0.4 mm). After 1 hour of exposure, water has yet to reach the full extent of the crack length. Therefore, Figures 3*(b)* and 4*(b)* indicate that although water traveled rapidly through cracks and free surface sorption behavior was observed below the notch bottom in cracked specimens, only a portion of the total crack length contributes as a free surface to water sorption while the remaining portion of the crack length inhibits sorption.

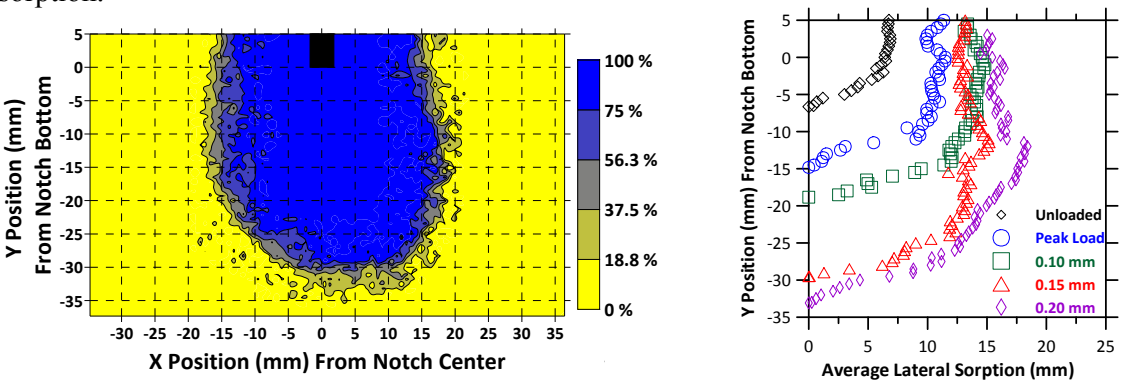

(a) *(b)*

Figure 4. *(a)* Absorption ratio contour plot for 0.15 mm CMOD specimen after 1 hour of ponding, and *(b)* Sorption profiles for WST specimen after 1 hour of ponding, under varying crack conditions

4. COMPARISON OF CRACK LENGTH AND SORPTION MEASUREMENTS

Figure 5*(a)* compares the CHM crack lengths to the maximum sorption depth after 1 hour of ponding in the cracked WST specimens. The broken line indicates equivalency. The single point which shows a higher maximum sorption depth than the crack length for the unloaded specimen (CHM crack length of 0 mm), while sorption in all cracked specimen has yet to reach the crack length after 1 hour of exposure to water.

As Figure 3*(b)* and 4*(b)* indicate a portion of the crack length behaves as a free surface while the remaining crack length inhibits water sorption. A possible source of this inhibition may be a lack of coalescence of the crack across a portion of the crack length. Figure 5*(b)* shows the difference between the CHM crack length and the maximum sorption depth for the specimens with varying crack lengths. For three of the cracked specimens tested (peak load, 0.15 mm CMOD, and 0.20 mm CMOD) this difference had a consistent range of 8 mm to 10 mm. Assuming the maximum sorption depth after 1 hour of exposure relates to the location of free surface behavior through the controlling sorption mechanisms, Figure 5*(b)* may indicate that a consistent length of the crack inhibits sorption. In other words, the results indicate the crack length consists of two portions, an apparent crack and an inhibiting crack. The apparent crack behaves approximately as a free surface in terms of sorption, while the inhibiting crack may have a consistent length and impedes sorption.

Further investigation is needed to determine if the sorption behavior in WST specimens with varying crack lengths can be directly related to fracture behavior using a constant inhibiting crack length. The 0.10 mm CMOD specimen results must also be investigated, although it is hypothesized that the rapidly increasing crack lengths at lower CMOD's (Figure 3*(c)*) may have affected this result. Additional testing will be undertaken to assess crack profiles and to verify the presence of coalesced cracks and isolated microcracks.

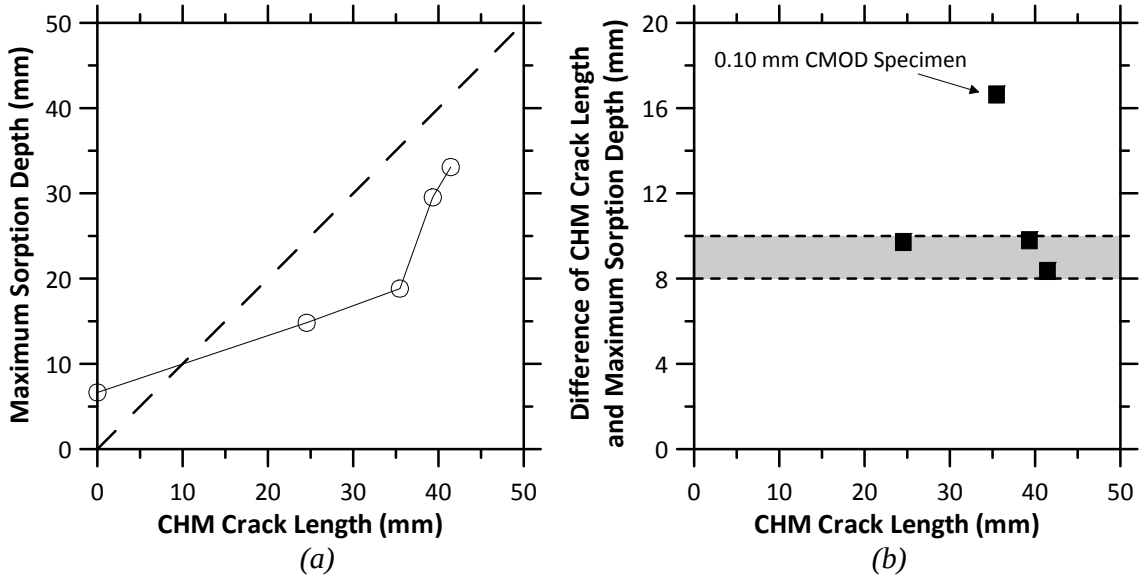

Figure 5. *(a)* Crack length from the CHM versus maximum sorption depth after 1 hour of water exposure, and *(b)* the difference in crack depth and maximum ingress depth for specimens with varying crack lengths.

5. SUMMARY

This paper presented results from x-ray absorption measurements of water sorption in WST specimens with varying crack lengths. The sorption behavior was used to quantify the impact of crack length on water sorption. It has been show that:

- As the crack mouth opening displacement increased the crack length increased and moisture reached deeper into the WST specimens after one hour of ponding.
- X-ray absorption measurements indicated that only a portion of the crack length has a free surface sorption behavior, while a consistent length of the total crack inhibits water sorption.

ACKNOWLEDGEMENTS

The first author gratefully acknowledges support received from the Otto Mønsted Fund and the Technical University of Denmark Department of Civil Engineering Travel Fund. The contents of this paper reflect the views of the authors, who are responsible for the accuracy of the data presented herein.

REFERENCES

[1] DS 2426, "Concrete – Materials – Rules for Application of EN 206-1 in Denmark"
[2] Comité Euro-International du Béton (CEB), "Durable Concrete Structures," Thomas Telford Services, Ltd. (1992)
[3] Østergaard, L., "Early-Age Fracture Mechanics and Cracking of Concrete - Experiments and Modeling," Ph.D Thesis, Technical University of Denmark, Lyngby, Denmark, 2003
[4] Skoček, J. & Stang, H., "Inverse Analysis of the Wedge Splitting Test," Engineering Fracture Mechanics, **75**(10) (2008) 3173-3188
[5] Ulfkjaer, J., Krenk, S. & Brincker, R., "Analytical Model for Fictitious Crack Propagation in Concrete Beams," Journal of Engineering Mechanics, **121**(1) (1995) 7-15
[6] Olesen, J., "Fictitious Crack Propagation in Fiber-Reinforced Concrete Beams," Journal of Engineering Mechanics, **127**(3) (2001) 272-280
[7] Skoček, J. & Stang, H., "Application of Optical Deformation Analysis System on Wedge Splitting Test and its Inverse Analysis, Submitted to Computational Materials Science (2008)
[8] Bentz, D., Geiker, M. & Hansen, K., "Shrinkage-reducing Admixtures and Early-age Desiccation in Cement Pastes and Mortars," Cement and Concrete Research, **31**(7) (2001) 1075-1085
[9] Hu, J. & Stroeven, P., "X-ray Absorption Study of Drying Cement Paste and Mortar," Cement and Concrete Research, **33**(3) (2003) 397-403
[10] Lura, P., Bentz, D., Lange, D., Kovler, K., Bentur, A. & Van Breugel, K., "Measurement of Water Transport from Saturated Pumice Aggregates to Hardening Cement Paste," Materials and Structures, **39**(293) (2006) 861-868
[11] Roels, S. & Carmeliet, J., "Analysis of Moisture Flow in Porous Materials using Microfocus X-Ray Radiography," Int. Journal of Heat and Mass Transfer, **49**(25-26) (2006) 4762-4772
[12] Weiss, J., Geiker, M. & Hansen, K., "Using X-Ray Absorption to Detect Fluid Ingress in Cracked Concrete," Submitted to Cement and Concrete Research (2008)
[13] GNI X-ray System, www.gni.dk (2006)
[14] ImageJ – Image Processing and Analysis in Java, www.rsbweb.nih.gov/ij/ (2008)
[15] Purdue Xray_Tiler ver 1.5, written in Image J, Compiling Date July 2008
[16] Couch, J. and Weiss, J., "Experimental Techniques for Calibrating and Processing x-ray Data Examining Moisture Ingress into Cementitious Materials," In Preparation